

## Photoexcitation Dynamics of Cyanate-ligated Ferric Heme Proteins Probed by Femtosecond Vibrational Spectroscopy<sup>#</sup>

Seongchul Park,<sup>†</sup> Jaeheung Park,<sup>†</sup> Joonkyung Jang,<sup>‡</sup> and Manho Lim<sup>†,\*</sup>

<sup>†</sup>Department of Chemistry and Chemistry Institute for Functional Materials, Pusan National University, Busan 609-735, Korea. \*E-mail: mhlím@pusan.ac.kr

<sup>‡</sup>Department of Nanomaterials Engineering, Pusan National University, Busan 609-735, Korea  
Received October 27, 2014, Accepted November 11, 2014, Published online February 20, 2015

The photoexcitation dynamics of cyanate-ligated ferric myoglobin (MbNCO) and hemoglobin (HbNCO) in D<sub>2</sub>O at 293 K after excitation with a visible pulse was investigated by probing the anti-symmetric stretching ( $\nu_1$ ) mode of the NCO<sup>-</sup> ion bound to Mb or Hb using femtosecond vibrational spectroscopy. The  $\nu_1$  mode of NCO in MbNCO or HbNCO in D<sub>2</sub>O shows one absorption feature near 2158 cm<sup>-1</sup>, which is similar to that of the free anion in D<sub>2</sub>O (2160 cm<sup>-1</sup>). The absorption feature of MbNCO was described by two absorption bands, *i.e.*, one major band (90%) peaked at 2157 cm<sup>-1</sup> with a full width at half maximum (FWHM) of 11 cm<sup>-1</sup> and a minor band (10%) at 2143 cm<sup>-1</sup> with an FWHM of 12 cm<sup>-1</sup>. In HbNCO, the major (82%) and minor (18%) bands are at 2159 (FWHM of 14 cm<sup>-1</sup>) and 2145 cm<sup>-1</sup> (FWHM of 14 cm<sup>-1</sup>), respectively. The major and minor bands were attributed to the high- and low-spin heme complexes, respectively. The photoexcited MbNCO and HbNCO undergo a rapid electronic relaxation with a time constant smaller than 0.4 ps, followed by thermal relaxation with a time constant of 8 ± 1 ps. No measurable absorption band for the photodeligated NCO<sup>-</sup> was detected, indicating that the photodeligation quantum yield of NCO<sup>-</sup>-bound ferric heme proteins is negligible. The characteristics of the thermal and electronic relaxations are independent of both the excitation wavelengths used (575 and 400 nm) and heme proteins probed (Mb and Hb). Although the interaction between the cyanate and Fe<sup>3+</sup> of the heme in Mb and Hb may be weak as suggested by the negligible shift in the band position of the cyanate upon ligand binding, the photodissociation of NCO<sup>-</sup> by a visible pulse is not significant. This finding is consistent with the negligible photodeligation observed for most of the other anion-ligated ferric heme proteins.

**Keywords:** Femtosecond infrared spectroscopy, Thermal relaxation, Photoexcitation dynamics, Cyanate ion, Heme proteins

### Introduction

Myoglobin (Mb) and hemoglobin (Hb) are typical heme proteins that contain a heme prosthetic group and are involved in O<sub>2</sub> storage and transport, respectively. They have been widely studied as model systems to investigate the relationship among protein structure, function, and dynamics.<sup>1</sup> The Fe atom in the heme of these proteins is five-coordinated; the sixth coordination site is available for various exogenous ligands. For example, ferrous heme proteins (with Fe<sup>2+</sup>) bind neutral ligands, such as O<sub>2</sub>, NO, and CO, whereas ferric heme proteins (with Fe<sup>3+</sup>) bind anionic ligands.<sup>2</sup> The binding and releasing of these ligands play a critical role in numerous biological functions;<sup>2,3</sup> knowledge of the heme-binding characteristics of the ligands is thus essential to understand fully the functioning mechanism of these proteins. The binding characteristics of the ligands are controlled by the protein conformation, which can change on a picosecond time-scale; its binding time constant can be faster than picoseconds. Thus, time-resolved spectroscopy has been utilized to investigate the binding dynamics

and conformational changes initiated by the ligand release after photodeligation of the ligated proteins.<sup>4–13</sup> When the ligated ferrous heme proteins were excited by the Soret or *Q* bands in the visible region, the photodeligation was found to proceed on a femtosecond time-scale with a significant quantum yield (QY).<sup>4,14</sup> Therefore, ligated ferrous heme proteins have been widely studied using a diverse range of experimental and theoretical methods to understand the ultrafast dynamics of ligand binding as well as the structural changes invoked in the ferrous protein by the ligand release.<sup>4–13</sup>

Unlike the dynamics of ligand binding to ferrous hemes, that to ferric hemes has been rarely reported.<sup>3,15,16</sup> Recently, CN<sup>-</sup>-bound heme proteins have been investigated after photoexcitation of the heme using transient visible and/or IR absorption spectroscopic methods.<sup>3,16,17</sup> According to these studies, the CN<sup>-</sup>-ligated heme proteins are photostable and not photodeligated by a visible photon. A more recent study on N<sub>3</sub><sup>-</sup>-ligated Mb (MbN<sub>3</sub>) has also shown that MbN<sub>3</sub> is not photodeligated upon visible excitation.<sup>15</sup> When photoexcited, MbN<sub>3</sub> was found to undergo a rapid electronic relaxation and to be thermally excited in the ground electronic state. The electronic relaxation was found to increase the population in the energetically higher high-spin (HS) state, which rapidly relaxes back

<sup>#</sup> This paper is dedicated to Professor Kwan Kim on the occasion of his honorable retirement.

to the lower-energy low-spin (LS) state.<sup>15</sup> This finding suggests that MbN<sub>3</sub> undergoes a rapid spin transition upon photoexcitation. As anion-ligated heme proteins are considered to be photostable, the ligand-binding dynamics may not be probed by analyzing the transient spectra after photoexcitation of the ligated protein. However, the transition between different energy states, i.e., HS-to-LS transition, can be probed by photoexcitation of the ligated protein.

Although anion-ligated heme proteins have been reported to be photostable, the studies of Zeng *et al.*, based on continuous-wave Raman, have shown that that CN<sup>-</sup>-ligated ferric Mb (MbCN) is photodeligated with a QY of 0.75, and that most of the deligated CN<sup>-</sup> rebinds geminately with a time constant of 3.6 ps.<sup>18</sup> The authors of the study concluded that a negligible amount of the deligated CN<sup>-</sup> escapes into the solution, because the escape rate is ca. 10<sup>4</sup> times slower than its geminate-rebinding (GR) rate, i.e., the detection of solvated CN<sup>-</sup> is practically impossible.<sup>18</sup> In these circumstances, the deligated ligand transiently builds up enough population in the heme pocket, despite its small amount in solution. Therefore, provided that the deligated ligand in the heme pocket has a different vibrational absorption, it can be readily probed by transient IR spectroscopy. Indeed, a recent time-resolved IR (TRIR) spectroscopic study on photoexcited MbCN showed a transient absorption appearing immediately after photoexcitation and decay with a time constant of 3.6 ps.<sup>18</sup> The transient absorption was red-shifted by 30 cm<sup>-1</sup> from the absorption band in equilibrium. The absorption was attributed to either the deligated CN<sup>-</sup> in the heme pocket or vibrationally excited CN ligand in MbCN. If the former is true, the GR time constant is expected to be 3.6 ps; if the absorption arises from a vibrationally excited CN ligand in MbCN, then its anharmonicity and vibrational relaxation time (*T*<sub>1</sub>) are 30 cm<sup>-1</sup> and 3.6 ps, respectively. It is thus critical to determine the anharmonicity and *T*<sub>1</sub> of CN in MbCN to properly assign the transient absorption.<sup>19</sup> However, these have not been measured due to the extremely weak extinction coefficient of the CN stretching mode. Instead, other anions, with favorable extinction coefficients, were investigated to characterize the photoexcitation dynamics of anion-ligated ferric heme proteins.<sup>19,20</sup> According to the recent measurements of the vibrational relaxation of NCO<sup>-</sup> and NCS<sup>-</sup> bound to ferric heme proteins, the *T*<sub>1</sub> value and anharmonicity of the anti-symmetric stretching ( $\nu_1$ ) mode of NCO in the NCO<sup>-</sup>-ligated Mb (MbNCO) and Hb (HbNCO) are about the same, i.e., 2.5 ± 0.3 ps and 19 ± 1 cm<sup>-1</sup>, respectively; those of NCS in the NCS<sup>-</sup>-ligated Mb and Hb are 6.9 ± 0.5 and 23 ± 1 cm<sup>-1</sup>, respectively.<sup>19</sup> Having determined these vibrational spectroscopic parameters, we can properly analyze the transient IR spectra of the photoexcited NCO<sup>-</sup> or NCS<sup>-</sup>-ligated heme proteins after excitation with a visible pulse. The *T*<sub>1</sub> value and anharmonicity of NO bound to various heme proteins have been thus measured to properly assign the transient IR signals of NO-ligated heme proteins after photoexcitation of the ligated proteins.<sup>11,21,22</sup>

In this study, we probed the photoexcitation dynamics of MbNCO and HbNCO in D<sub>2</sub>O after excitation with an intense

visible pulse at 575 or 400 nm using femtosecond IR spectroscopy. The photoexcited MbNCO and HbNCO relax via a rapid electronic transition to the ground electronic state with a time constant smaller than 0.4 ps, producing thermally excited low-frequency vibrational modes that anharmonically couple with the  $\nu_1$  mode of the cyanate in MbNCO and HbNCO. The thermal modes decay with a time constant of 8 ± 1 ps. The photoexcitation dynamics of the cyanate-ligated heme proteins was found to be independent of the excitation wavelength (400 and 575 nm) or heme proteins (Mb and Hb) used. When excited in the visible region, the cyanate-ligated heme proteins are photostable, and the electronic relaxation is very efficient in dumping the excess energy into thermal energy.

## Experimental

**Sample Preparation.** Sample preparation was described previously.<sup>19</sup> Briefly, reagent-grade NaNCO and Na<sub>2</sub>S<sub>2</sub>O<sub>4</sub> as well as lyophilized horse-skeleton Mb and human Hb were purchased from Sigma-Aldrich Co. (St. Louis, MO, USA) and used as received. The heme protein was dissolved in D<sub>2</sub>O buffered with 0.1 M potassium phosphate (pD = 7.4), and the protein solution was centrifuged to remove any protein aggregate and undissolved impurity. NCO<sup>-</sup>-stock solution was also prepared in the phosphate D<sub>2</sub>O buffer solution. A small amount of NCO<sup>-</sup>-stock solution was added to the filtered protein solution to prepare MbNCO or HbNCO. Because the binding constant of NCO<sup>-</sup> to the heme protein is finite (450–460 at 293 K),<sup>19</sup> the final solution is a mixture of ligated protein, unligated protein, and free anion. The final concentrations of the heme and anions were 10 and 20 mM, respectively, resulting in that about 85% of the added protein was ligated. As the heme concentration of Hb, which has four heme units, is four times that of Mb, the concentration of heme was used instead of that of Hb for the sake of comparison with Mb. The sample was loaded in a gas-tight 27- $\mu$ m path-length sample cell with two CaF<sub>2</sub> windows. The sample cell was rotated sufficiently quickly so that each laser pulse excited a fresh volume of the sample. D<sub>2</sub>O was used to avoid the strong water absorption in the spectral region of interest. Even with the deuterated solution, a short path length was required because of the strong D<sub>2</sub>O absorption near 2160 cm<sup>-1</sup>, where the Fe(III)NCO adduct also absorbs. The integrity of the sample was checked by UV-Vis and FT-IR spectroscopy. The temperature of the sample was maintained at 293 ± 1 K.

**Femtosecond Infrared Spectrometer.** The femtosecond infrared spectrometer used here was described previously.<sup>10,22</sup> Briefly, two optical-parametric amplifiers (OPAs), pumped by a Ti:sapphire amplifier (110 fs pulses at 800 nm with a repetition rate of 1 kHz), were used to generate a visible-pump pulse with 3  $\mu$ J of energy and a mid-IR probe pulse. The probe pulse was generated by difference frequency mixing of the signal and idler pulses of one OPA. The visible pulse at 575 nm was produced by frequency doubling of the signal pulse from the other OPA, and that at 400 nm by the second harmonic generation of the amplifier output at 800 nm. The generated

mid-IR pulse is sufficiently spectrally broad ( $\sim 170\text{ cm}^{-1}$ ) to probe the spectral range of interest without tuning the spectrum to another wavelength. Only a small portion of the intense IR pulse was used as a probe pulse not to perturb the sample while probing. The isotropic-absorption spectrum was obtained by setting the polarization of the pump pulse at the magic angle ( $54.7^\circ$ ) to that of the probe pulse by rotating the polarization of the pump pulse using a half waveplate. The pumped and unpumped absorption signals were collected quasi-simultaneously by blocking the pump beam at 0.5 kHz using a chopper.<sup>10,22</sup> After passing through the sample, the spectrally broad probe pulse was recorded by a  $\text{N}_2(\text{l})$ -cooled 64-element HgCdTe array detector attached in a 320-mm monochromator with a grating of 150 l/mm. The spectral resolution of the probe pulse near  $2160\text{ cm}^{-1}$  was  $1.54\text{ cm}^{-1}$  per pixel. The pump-induced change in the absorbance of the sample,  $\Delta A$ , was obtained by subtracting the unpumped absorbance from the pumped one and recorded in mOD unit ( $1\text{ mOD} = 1 \times 10^{-3}\text{ OD}$ ). The instrument response function was ca. 0.3 ps.

### Results and Discussion

Figure 1 shows the vibrational absorption bands of the  $\nu_1$  mode of  $\text{NCO}^-$  as a free ion in  $\text{D}_2\text{O}$  buffer solution and as a bound ligand in HbNCO and MbNCO in the same buffer solution at 293 K. As only part of the added anion is ligated, the absorption from the protein solution has a contribution from both the free anion and the ligand bound to the protein. Therefore, the absorption features for the  $\text{NCO}^-$  bound to the heme proteins were obtained by carefully subtracting the absorption contribution from the free anion in solution, which was calculated from the known equilibrium constant.<sup>19,23</sup> While the absorption feature for the free anion was described by a single band, that for the bound ion is characterized by two bands, which were described by Gaussian functions. The major band (90%) of MbNCO was peaked at  $2057\text{ cm}^{-1}$  with a full width at half maximum (FWHM) of  $11\text{ cm}^{-1}$ , and the minor band (10%) peaked at  $2043\text{ cm}^{-1}$  with an FWHM of  $12\text{ cm}^{-1}$ . In the case of HbNCO, the major band (82%) was centered at  $2059\text{ cm}^{-1}$  with an FWHM of  $14\text{ cm}^{-1}$ , and the minor one (18%) was at  $2045\text{ cm}^{-1}$  with an FWHM of  $14\text{ cm}^{-1}$ . The minor (with 10–18% population) and major bands were red-shifted by 15–17 and 1–3  $\text{cm}^{-1}$ , respectively, from the absorption band of the free anion in  $\text{D}_2\text{O}$  at  $2160\text{ cm}^{-1}$ .<sup>19</sup> The absorption bands of the bound anion are narrower than those of the free anion (FWHM of  $16\text{ cm}^{-1}$ ),<sup>19</sup> suggesting that the protein environment near the ligand is slightly more homogeneous than water solution. The narrower band in Mb compared to that in Hb indicates that the tetrameric Hb structure increases the inhomogeneity of the ligand environment. The recovered absorption feature is consistent with the bleach in the transient absorption, where only the bound anion contributes to the transient signal (vide infra). Although the protein solution is a mixture of free anion, ligated protein, and unligated protein, the free anion cannot be excited by the visible pulse, and thus only

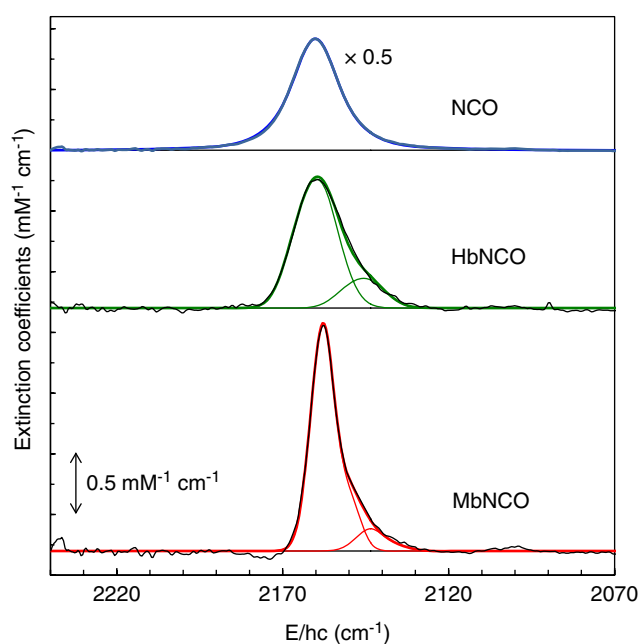


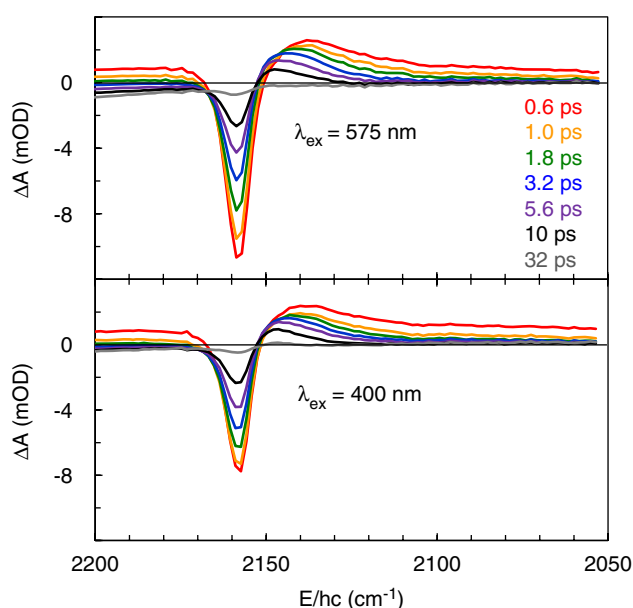
**Figure 1.** Equilibrium-absorption spectra of the  $\nu_1$  mode of  $\text{NCO}^-$  (top panel, blue) in  $\text{D}_2\text{O}$  buffer,  $\text{NCO}^-$  in HbNCO (middle panel, green), and  $\text{NCO}^-$  in MbNCO (bottom panel, red) at 293 K. The absorption bands for the heme complexes were obtained by subtracting the free  $\text{NCO}^-$  contribution from the data obtained for the mixture of protein and anion. The  $\text{NCO}^-$  band in the heme complexes was decomposed into two absorption bands (thin lines), which can be assigned to high-spin (main band) and low-spin (minor band) complexes. The thick and black thin lines represent fit and background-subtracted data, respectively. For the sake of visualization, the spectrum for  $\text{NCO}^-$  in  $\text{D}_2\text{O}$  was scaled down to a half ( $\times 0.5$ ).

the ligated heme protein shows the transient signal in the  $\nu_1$  mode of  $\text{NCO}^-$  after visible excitation. In contrast, the transient absorption signal in the IR pump–IR probe experiments results from a contribution of both the free anion and that bound to the heme.<sup>19</sup> Consequently, the equilibrium spectrum consistent with the transient signal from visible pump–IR probe experiment is more reliable. The integrated extinction coefficients for the  $\nu_1$  mode of  $\text{NCO}^-$  in both MbNCO and HbNCO were determined to be  $22 \pm 2\text{ mM}^{-1}\text{ cm}^{-1}$ , which is about half of that for the free  $\text{NCO}^-$  in  $\text{D}_2\text{O}$  ( $39 \pm 2\text{ mM}^{-1}\text{ cm}^{-1}$ ). These values are significantly smaller than those reported in our previous study; however, we should remark that an error was found in our previous calculations.<sup>19</sup>

When an anion binds the heme iron, the iron forms an LS, an HS, or a mixture of HS and LS complexes, depending on the strength of the ligand field. For example, if ligated with the strong field-ligand  $\text{CN}^-$ , MbCN exists as an LS complex, while MbF exists as an HS complex, if ligated with the weak field-ligand  $\text{F}^-$ .<sup>24</sup> In the case of  $\text{NCO}^-$ , the heme complex was found to exist mainly in the HS form, but the LS form cannot be neglected at room temperature, i.e., MbNCO and HbNCO were reported to exist as an LS form with 10% and 18% population at  $20^\circ\text{C}$ , respectively.<sup>25–27</sup> These values are identical to the magnitude of the red-shifted minor band in the

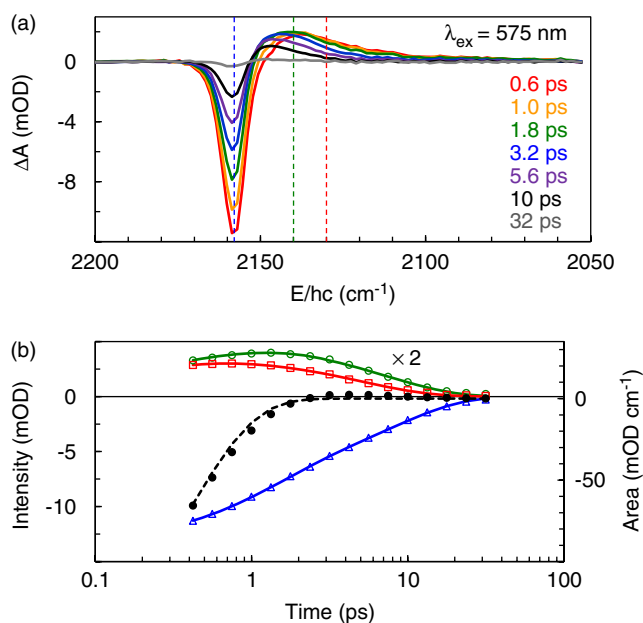
absorption band of NCO in MbNCO and HbNCO. The intensities of the vibrational bands for a ligand in a ligated-heme protein have been used to account for the populations of the corresponding species.<sup>4</sup> Thus, the intensity of the minor band likely reflects the population of the minor species. Therefore, we assigned the red-shifted minor and the major bands to the LS and HS complexes of NCO<sup>-</sup>-ligated heme proteins, respectively. An LS complex arises from the stronger interaction between the ligand and the transition metal bound to the ligand compared to those in an HS complex. The  $\nu_1$  mode of NCO of MbNCO and HbNCO in the LS and HS complexes are red-shifted by 15–17 and 1–3 cm<sup>-1</sup>, respectively, compared to that of the free anion. Clearly, stronger interaction leads to a more significant red-shift in the  $\nu_1$  mode. The bonding interaction in the LS complex cannot be several times larger than that in the HS complex. If the red-shift is roughly proportional to the strength of the bonding interaction, the shift of the HS complex from the free ligand should be larger than 3 cm<sup>-1</sup>. Thus, the band position of NCO<sup>-</sup> in the heme pocket is expected to be blue-shifted from that in water solution.

Figure 2 shows representative TRIR spectra of the  $\nu_1$  band of NCO in MbNCO after excitation with a 575- or a 400-nm pulse. Except the slightly smaller magnitude in the transient signal obtained by pumping with 400 nm, the TRIR spectra are virtually identical. We observed bleach signals similar to those of the inverted equilibrium spectrum as well as a broad red-shifted absorption, which narrows toward the blue wavelength region as the pump–probe delay increases. Although the minor band is not apparent in the bleach due to the overlap with the new absorption, the bleach was assumed to have equal contribution from minor and major bands. In addition to the



**Figure 2.** Representative transient absorption spectra near the  $\nu_1$  mode of NCO in MbNCO in D<sub>2</sub>O at 293 K after excitation by a 575- (top panel) or a 400-nm (bottom panel) pulse. The pump–probe time delays (color-coded) are 0.6, 1.0, 1.8, 3.2, 5.6, 10, and 32 ps.

bleach and absorption, the transient signals are on top of a broad background, which is initially positive and becomes negative as the pump–probe delay increases. The initial positive signal is known to arise from the cross-phase modulation during the overlap of pump and probe pulses in the sample.<sup>28</sup> The negative signal at the later time results from an increase in the solvent temperature that weakens the hydrogen bonding of D<sub>2</sub>O, which in turn causes the absorption band of D<sub>2</sub>O to shift toward higher energies. Because the  $\nu_1$  band of NCO is located in a lower energy side of the D<sub>2</sub>O absorption, as the D<sub>2</sub>O absorption band shifts to higher energies, the background becomes negative. The increase of the background toward the negative signal has been used as a measure of the thermal-energy transfer. The background changed with a time constant of 6–10 ps and sustained the negative value for tens of picoseconds; this is consistent with previously determined values in heme systems.<sup>29,30</sup> For the sake of analysis, the broad background was subtracted from the data of the transient signal related to the  $\nu_1$  mode. Figure 3(a) shows the background-subtracted data pumped with a 575-nm pulse. As the pump wavelength hardly affects the transient signal, hereafter we



**Figure 3.** (a) Representative transient absorption spectra (pumped at 575 nm) of the  $\nu_1$  mode of NCO<sup>-</sup> in MbNCO in D<sub>2</sub>O buffer obtained after subtracting the broad-background signal. The pump–probe time delays (color-coded) are 0.6, 1.0, 1.8, 3.2, 5.6, 10, and 32 ps. Dotted vertical lines mark the sampling position for the time-dependent change in the transient signal (see text for further details). (b) Time-dependent changes of the bleach at 2158 cm<sup>-1</sup> (open triangles), absorption at 2140 cm<sup>-1</sup> (open circles), and 2130 cm<sup>-1</sup> (open squares), and integrated area of the transient signal (filled circles, right ordinate); also in the figure, bleach and absorption (left ordinate). The time-dependent intensity changes are well described by an exponential function with two time constants (solid lines). Time-dependent area is well described by an exponential function with a time constant of 0.4 ps (dotted line). Time-dependent changes of the absorption were scaled ( $\times 2$ ) for the sake of visualization.

will discuss only the transient signal of MbNCO excited with a 575-nm pulse, unless stated otherwise. As displayed in Figure 3(a), the transient signal shows a bleach similar to the fundamental band due to the loss of population in the ground vibrational state of the ground electronic state. The new absorption in the transient signal typically arises from the fundamental band anharmonically coupled to the low-frequency mode, which is thermally excited due to a rapid electronic relaxation of the photoexcited state.<sup>31</sup> If the electronic relaxation of the photoexcited state produced a vibrationally excited  $\nu_1$  mode of NCO in MbNCO in the ground electronic state, a hot band at  $2138\text{ cm}^{-1}$  would appear that decays with a time constant of 2.6 ps.<sup>19</sup> However, no detectable hot band appears in the transient signal, indicating that the energy flow to the  $\nu_1$  mode of NCO in MbNCO during the electronic relaxation is very inefficient. If the photoexcited MbNCO were deligated, an absorption band corresponding to  $\text{NCO}^-$  in the heme pocket would appear. The absorption band for  $\text{NCO}^-$  in the heme pocket is not necessarily the same as that for  $\text{NCO}^-$  in  $\text{D}_2\text{O}$ . As mentioned above, because the weaker interactions between the anion and the heme iron, resulting in an HS complex, were less red-shifted from those in the  $\text{D}_2\text{O}$  solution, the absorption band for  $\text{NCO}^-$  in the heme pocket may be blue-shifted from the band in the  $\text{D}_2\text{O}$  solution. However, no absorption-like feature could be attributed to the deligated  $\text{NCO}^-$  in the heme pocket. Therefore, we concluded that the photodeligation QY after excitation with a visible pulse is negligible.

The time-dependent behavior of the bleach and the absorption was obtained by sampling the magnitude change of the corresponding signal.<sup>29</sup> When sampled at  $2158\text{ cm}^{-1}$  (the peak of the bleach), the bleach decayed with two time constants, e.g., 1.2 and 8.4 ps. When sampled at  $2140\text{ cm}^{-1}$ , the absorption grows with a time constant of 0.5 ps and decays with a time constant of 7.3 ps. The absorption sampled at  $2130\text{ cm}^{-1}$  grows with a time constant of 0.3 ps and decays with a time constant of 5.2 ps. As shown in Figure 3(b), the time constant for the transient absorption varied depending on the sampling position. Both the growth and decay times are reduced as the sampling position shifts toward the lower energy side. The integrated area of the transient signal rapidly decays to zero with a time constant of 0.4 ps (Figure 3(b)). As mentioned above, as the transient absorption arises from the fundamental band coupled with the low-frequency thermal mode, it has the same extinction coefficient as the fundamental band. Therefore, the negative value in the summed area shown in Figure 3(b) represents the population that has not yet reached the ground electronic state. Consequently, the decay with the time constant equal to 0.4 ps can be attributed to the relaxation time of the electronically excited state to the thermally excited ground electronic state. To properly obtain time constants for the thermal ( $\tau_t$ ) and electronic ( $\tau_e$ ) relaxation from these data, the transient signal was described by a three-state scheme as shown in Figure 4. Initially, a visible photon excites the molecule, and the excited molecule rapidly relaxes to the ground electronic state, producing a thermally excited ground

electronic state. The thermal state grows with  $\tau_e$  and decays with  $\tau_t$ . Based on our data, no signal could be assigned to the excited state, suggesting that the  $\nu_1$  vibrational mode in the excited electronic state is outside of the probed-spectral window shown. As the thermal state cools down, its band narrows and blue shifts toward the fundamental band. Our entire set of data was globally fit to the three-state scheme. As shown in Figure 5, the proposed scheme correctly reproduces the data with the two time constants  $\tau_e$  and  $\tau_t$ . The recovered time

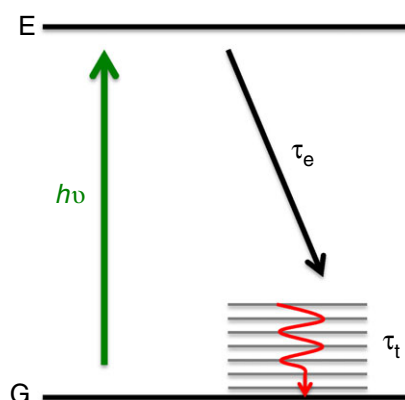


**Figure 4.** A kinetic scheme that describes the transient absorption spectra. G and E represent the ground and excited electronic states, respectively;  $\tau_e$  and  $\tau_t$  represent the electronic and thermal relaxation time, respectively.

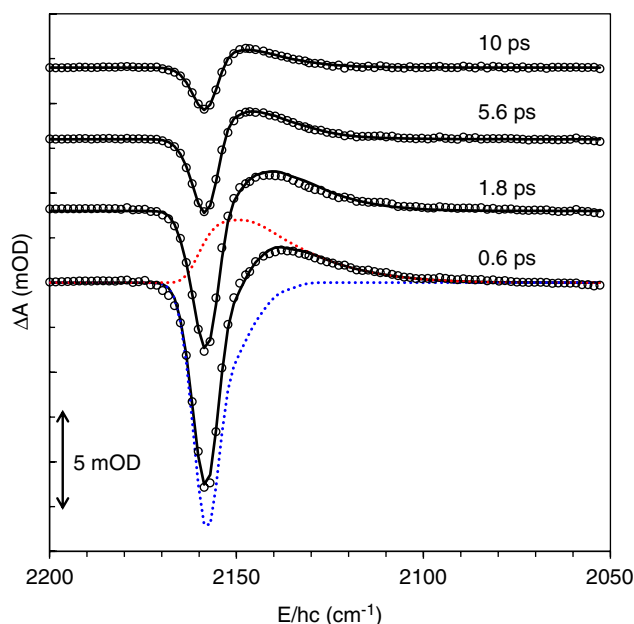


**Figure 5.** Global fit (solid lines) of the transient spectra (open circles) with the three-state model with a scaled-equilibrium spectrum (negative-going dotted line) and evolving absorption spectrum (positive-going dotted line). The evolving absorption narrows and shifts toward blue wavelength as the pump-probe delay increases. The pump-probe time delays are 0.6, 1.8, 5.6, and 10 ps (bottom to top).



constants are 0.5 and 8.2 ps, respectively, for the transient spectra of MbNCO excited with 575 nm. When excited with 400 nm, these time constants are 0.4 and 9.1 ps, respectively. The transient spectra of HbNCO excited with 575 nm showed a very similar behavior to those of MbNCO. Using the same approach, we determined the time constants to be 0.4 and 7.4 ps. Considering that the time resolution of our instrument is ca. 0.3 ps, a  $\tau_c$  value of 0.4–0.5 ps implies that the electronic relaxation time is shorter than 0.4 ps. The thermal relaxation time is thus likely to be  $8 \pm 1$  ps. The observed thermal relaxation time represents the relaxation of excess thermal energy deposited into heme. It is consistent with the previously reported relaxation time of 5–10 ps obtained for various heme proteins observed after visible excitation.

According to the assignment of the electronic absorption spectrum of ligated Hb,<sup>32</sup> the HS ferric Hb complex shows the Soret and  $Q_0$  bands at 405 and at 540 nm, respectively. Both bands arise from the porphyrin  $\pi \rightarrow \pi^*$  transitions. A vibronic  $Q$  band ( $Q_v$ ) peaked at 500 nm in the HS complex will be ignored hereafter, as it is not relevant to our discussion. The HS ferric complex also absorbs at 580 nm; this was assigned to the porphyrin ( $\pi$ ) $\rightarrow$ Fe ( $d_{xz}$ ,  $d_{yz}$ ) transitions.<sup>32</sup> In the case of the LS Hb ferric complex, the Soret and  $Q_0$  bands are peaked at 422 and 575 nm, respectively. The electronic absorption spectrum of ferric Mb is virtually identical to that of ferric Hb and it was assigned to the same transitions as those of ferric Hb. According to this, both the 400- and 575-nm excitations invoke only the porphyrin  $\pi \rightarrow \pi^*$  transitions in the LS MbNCO. However, the 575-nm excitation can cause a ligand-to-metal charge transfer as well as the porphyrin  $\pi \rightarrow \pi^*$  transitions in the HS complex. Clearly, for the majority of the NCO<sup>-</sup>-ligated ferric-heme complexes, i.e., HS complexes, the 575-nm pulse can cause a different transition from the 400-nm pulse. The characteristics of the transient absorption signals, independent of pump wavelengths of 400 and 575 nm, indicate that the excited states, whether a porphyrin  $\pi^*$  or charge-transfer state, show similar electronic relaxation behavior.

During the photoexcitation of heme proteins, the photon energy is absorbed by the heme and can be rapidly converted to heat, causing the vibrational temperature of the heme to rise significantly. For example, the vibrational temperature was calculated to increase by as much as 500 K, when cytochrome *c* was pumped by a 420-nm photon.<sup>33</sup> As the hot heme is surrounded by the protein matrix, the dissipation of excess heat was described by sequential transport; i.e., as the chromophore cools down, the temperature of the protein matrix increases and decays, and the protein cools down as the heat diffuses into solvent. The temperature of the hot heme was found to decay with a double exponential function at short times and to roll over to a function  $t^{-3/2}$  at the diffusion limit.<sup>34</sup> Furthermore, a biomolecule with a photoexcited chromophore was found to reach the thermal steady-state on a picosecond time-scale.<sup>34</sup> The thermal band in our data arises from the thermally excited low-frequency modes of the heme, and thus the magnitude of the transient absorption reflects the heme temperature. In

contrast, the change in the amide band after photoexciting the heme proteins probes the protein temperature. Therefore, the protein temperature can be followed by carefully measuring the changes in the amide band. The temperature change of the heme protein likely occurs on a time-scale ranging between a few picoseconds and tens of picoseconds; this is consistent with the thermal relaxation of 20–40 ps of the protein matrix estimated from molecular dynamics simulations.<sup>33</sup>

## Conclusion

We obtained the transient IR spectra of the  $\nu_1$  bands of NCO in MbNCO and HbNCO at 293 K after excitation with a 575- or a 400-nm pulse. The transient spectra show an instantaneous bleach that decays with the pump–probe delay and an absorption that decays after initial growth. The absorption band, initially broad and red-shifted from the fundamental band, shifts toward blue wavelength and narrows; this behavior is typical of a fundamental band anharmonically coupled with thermally excited low-frequency modes. The transient spectra showed no signature for the absorptions arising from the deligated NCO<sup>-</sup> in the heme pocket or the vibrationally excited  $\nu_1$  mode of NCO in the ligated heme proteins; this suggests that, during the electronic relaxation, the energy flow to the  $\nu_1$  mode is inefficient and that the photodeligation QY of the NCO<sup>-</sup>-ligated heme protein by a visible pulse is negligible. The transient spectra were well described by a three-state scheme, i.e., a ground electronic state, an excited electronic state, and a thermally excited ground electronic state. From a global fitting of the transient spectra to this three-state scheme, we obtained a value of <0.4 ps for the electronic relaxation time of the excited electronic state of the NCO<sup>-</sup>-ligated heme protein after visible excitation and a value of  $8 \pm 1$  ps for the relaxation time of excess thermal energy deposited into heme. The NCO<sup>-</sup>-ligated Mb and Hb appear to be photostable, and the excess energy by a visible photon is efficiently dumped out as thermal energy after a rapid electronic relaxation.

**Acknowledgments.** This work was supported by the National Research Foundation of Korea (NRF) grant funded by the Korea government (MSIP) (NRF-2014R1A2A2A01002456, NRF-2014R1A4A1001690, NRF-2013S1A2A2035406). This work was also supported by MSIP and PAL, Korea.

## References

1. B. A. Springer, S. G. Sligar, J. S. Olson, G. N. Phillips Jr., *Chem. Rev.* **1994**, *94*, 699.
2. E. Antonini, M. Brunori, Hemoglobin and Myoglobin in their Reactions with Ligands (Frontiers of Biology, Vol. 21), North-Holland, **1971**, p. 436.
3. J. Helbing, L. Bonacina, R. Pietri, J. Bredenbeck, P. Hamm, F. van Mourik, F. i. Chaussard, A. Gonzalez-Gonzalez, M. Chergui, C. Ramos-Alvarez, C. Ruiz, J. Lopez-Garriga, *Biophys. J.* **2004**, *87*(3), 1881.

4. A. Ansari, J. Berendzen, D. K. Braunstein, B. R. Cowen, H. Frauenfelder, M. K. Hong, I. E. T. Iben, J. B. Johnson, P. Ormos, T. B. Sauke, R. Scholl, A. Schulte, P. J. Steinbach, J. Vittitow, R. D. Young, *Biophys. Chem.* **1987**, *26*, 337.
5. R. H. Austin, K. W. Beeson, L. Eisenstein, H. Frauenfelder, I. C. Gunsalus, *Biochemistry* **1975**, *14*, 5355.
6. D. A. Chernoff, R. M. Hochstrasser, W. A. Steele, *Proc. Natl. Acad. Sci. U. S. A.* **1980**, *77*, 5606.
7. P. A. Cornelius, R. M. Hochstrasser, A. W. J. Steele, *Mol. Biol.* **1983**, *163*, 119.
8. E. R. Henry, J. H. Sommer, J. Hofrichter, W. A. J. Eaton, *Mol. Biol.* **1983**, *166*(3), 443.
9. J. Kim, J. Park, T. Lee, Lim, M. *J. Phys. Chem. B* **2012**, *116*(46), 13663.
10. S. Kim, G. Jin, Lim, M. *J. Phys. Chem. B* **2004**, *108*(52), 20366.
11. S. Kim, J. Park, T. Lee, Lim, M. *J. Phys. Chem. B* **2012**, *116*(22), 6346.
12. J. W. Petrich, J. C. Lambry, K. Kuczera, M. Karplus, C. Poyart, J. L. Martin, *Biochemistry* **1991**, *30*, 3975.
13. A. Szabo, *Proc. Natl. Acad. Sci. U. S. A.* **1978**, *75*(5), 2108.
14. X. Ye, A. Demidov, P. M. Champion, *J. Am. Chem. Soc.* **2002**, *124*(20), 5914.
15. J. Helbing, *Chem. Phys.* **2012**, *396*, 17.
16. J. Kim, J. Park, S. A. Chowdhury, Lim, M. *Bull. Korean Chem. Soc.* **2010**, *31*(12), 3771.
17. F. Gruia, M. Kubo, X. Ye, P. M. Champion, *Biophys. J.* **2008**, *94*(6), 2252.
18. W. Zeng, Y. Sun, A. Benabbas, P. M. Champion, *J. Phys. Chem. B* **2013**, *117*(15), 4042.
19. S. Park, J. Park, H.-W. Lin, Lim, M. *Bull. Korean Chem. Soc.* **2014**, *35*(3), 758.
20. M. Maj, Y. Oh, K. Park, J. Lee, K.-W. Kwak, M. Cho, *J. Chem. Phys.* **2014**, *140*(23), 235104/235101.
21. J. Park, T. Lee, M. Lim, *Chem. Phys.* **2013**, *422*, 107.
22. J. Park, T. Lee, J. Park, Lim, M. *J. Phys. Chem. B* **2013**, *117*(10), 2850.
23. A. Jain, R. J. Kassner, *J. Biol. Chem.* **1984**, *259*(16), 10309.
24. M. Sono, J. H. Dawson, *J. Biol. Chem.* **1982**, *257*(10), 5496.
25. D. W. Smith, R. J. P. Williams, *Biochem. J.* **1968**, *110*(2), 297.
26. K. C. Cho, J. J. Hopfield, *Biochemistry* **1979**, *18*(26), 5826.
27. R. W. Noble, A. DeYoung, D. L. Rousseau, *Biochemistry* **1989**, *28*(12), 5293.
28. A. Lapini, S. M. Vazquez, P. T. Touceda, M. Lima, *J. Mol. Struct.* **2011**, *993*(1–3), 470.
29. M. Li, J. Owrutsky, M. Sarisky, J. P. Culver, A. Yodh, R. M. Hochstrasser, *J. Chem. Phys.* **1993**, *98*(7), 5499.
30. T. Lian, B. Locke, Y. Kholodenko, R. M. Hochstrasser, *J. Phys. Chem.* **1994**, *98*(45), 11648.
31. P. Hamm, S. M. Ohline, W. Zinth, *J. Chem. Phys.* **1997**, *106*(2), 519.
32. W. A. Eaton, J. Hofrichter, *Methods Enzymol.* **1981**, *76*, 175.
33. E. R. Henry, W. A. Eaton, R. M. Hochstrasser, *Proc. Natl. Acad. Sci. U. S. A.* **1986**, *83*(23), 8982.
34. P. Li, P. M. Champion, *Biophys. J.* **1994**, *66*(2, Pt. 1), 430.